

# System Design and Optimization of Optically Amplified WDM-TDM Hybrid Polarization-Insensitive Fiber-Optic Michelson Interferometric Sensor

Wuu-Wen Lin, Shih-Chu Huang, Jiunn-Song Tsay, and Shorn-Chien Hung

**Abstract**—In this paper, we investigate the optically amplified time-division-multiplexed (TDM) polarization-insensitive fiber-optic Michelson interferometric sensor (PIFOMIS) system using erbium-doped fiber amplifier (EDFA). The EDFA was named preamplifier, in-line amplifier or postamplifier, by the position it was located. We find that the preamplifier EDFA has limited usefulness because of its unstable amplification of the optical pulse trains. Both post- and in-line cases can work successfully in the TDM-PIFOMIS system. The amplitudes of the optical pulse trains are stable after amplified by the in-line EDFA, this is a significantly advantage of the optically amplified TDM-PIFOMIS system. The MPDS of the unamplified TDM-PIFOMIS system with an extinction ratio (ER) of 33 dB of the output pulse of the optical guide wave (OGW) modulator was  $2.4 \times 10^{-5}$  rad/(Hz) $^{1/2}$  at 1 kHz. For maintaining MPDS better than  $3.4 \times 10^{-5}$  rad/(Hz) $^{1/2}$  at 1 kHz, the allowable worst ER for the post- and in-line amplified system are 20 and 17.8 dB, respectively, and the corresponding input signal peak power should be larger than -20 and -25 dBm. While employing such two post- and two in-line EDFA's in the TDM-PIFOMIS system, the allowable loss of the sensor array is 47 dB. We analyze the phase-induced intensity noise (PIIN) of the optically amplified TDM-PIFOMIS system in detail and propose methods to reduce the PIIN. The output optical pulse of an intensity modulator with high ER is a key issue to minimize the PIIN and sensor crosstalk in the system. In order to reduce the system PIIN, complexity and cost, we suggest an optimum optically amplified WDM (wavelength-division multiplexing)-TDM hybrid PIFOMIS system with four wavelengths and four eight-sensor subarrays.

**Index Terms**—Erbium-doped fiber amplifier (EDFA), Faraday rotator mirror (FRM), Michelson interferometric sensor, phase-induced intensity noise (PIIN), time-division multiplexed (TDM), wavelength-division multiplexing.

## I. INTRODUCTION

Single-mode fiber-optic interferometric sensors (FOIS) have many advantages and have been developed for a wide range of applications [1]. An important feature of FOIS is its multiplexing capability [2]. Among different interferometric sensor multiplexing techniques, time-division multiplexing (TDM) has been shown to have low crosstalk and high sensitivity [3]. However, if sensors in the TDM configuration are constructed of regular single-mode fiber, fluctuation of the

sensor output occurs easily because of polarization-induced signal fading. To reduce the fading effect, polarization-insensitive fiber optic Michelson interferometer was proposed [4]. This interferometer includes two Faraday rotator mirrors (FRM) which can eliminate polarization fading by compensation of birefringence effect in a retraced fiber path [5]. Recently, we reported a TDM polarization-insensitive fiber optic Michelson interferometric sensor (TDM-PIFOMIS) system to overcome the polarization-induced fading by combining FRM with unbalanced Michelson interferometers and generating the interference signals by an optical path-matching compensation interferometer (CI) [6], [7]. The TDM-PIFOMIS system with the optical path-matching CI also shows that it can significantly reduce the phase-induced intensity noise (PIIN) [8]. The crosstalk analysis and system design of the TDM-PIFOMIS system were reported [7], [9].

For most fiber-optic sensor multiplexing schemes, the optical power budget limits both the length of lead fiber and the number of sensors. The UK Defence Research Agency has modeled the effect of placing EDFA's as a postamplifier and as a preamplifier within an optical hydrophone system [10]. Their conclusions showed that the number of sensors can be increased to six times of the unamplified system for the booster with 30 dB optical gain. Recently, an optically amplified TDM-PIFOMIS system using EDFA's as post- and in-line amplifiers was reported [11]. The influence of EDFA on the ER of amplified light pulse and the minimum phase detection sensitivity (MPDS) of the system was examined [11]. In this paper, we investigated the influence of the ER of the optical pulse from the OGW output, and the effect of the amplified spontaneous emission (ASE) of the EDFA in the optically amplified TDM-PIFOMIS system. We find that the MPDS of the system is primarily limited by the PIIN; therefore, it is important to theoretically analyze the PIIN of the system.

In the system design, we propose an optimum optically amplified WDM (wavelength-division-multiplexing)-TDM-PIFOMIS hybrid system to improve the MPDS and to reduce the complexity and the electrical power consumption.

## II. OPTICALLY AMPLIFIED TDM-PIFOMIS SYSTEM

### A. System Configuration and Experimental Setups

The optically amplified TDM-PIFOMIS system shown in Fig. 1 is composed of four main parts: the optical pulse gener-

Manuscript received December 15, 1998; revised October 26, 1999.

The authors are with Chung-Shan Institute of Science and Technology, Kaohsiung 813, Taiwan, R.O.C.

Publisher Item Identifier S 0733-8724(00)02186-1.

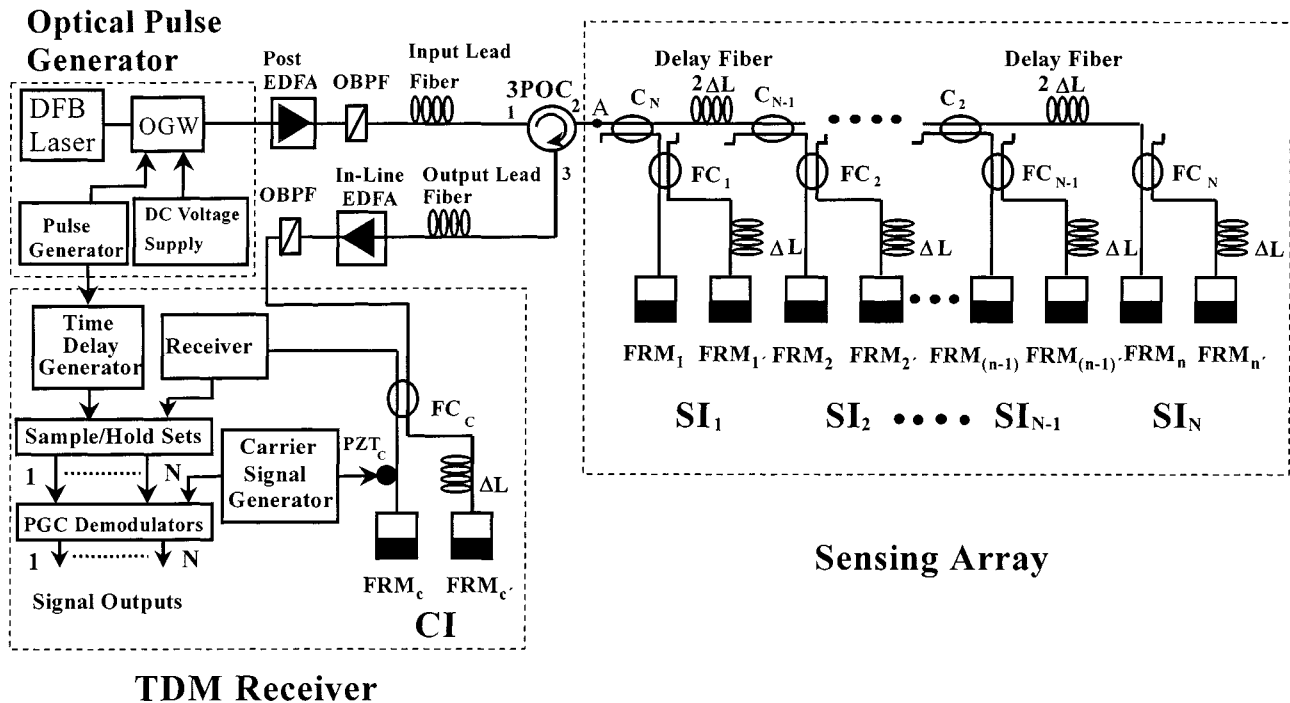


Fig. 1. The optically amplified TDM-PIFOMIS system.

ator, lead fiber subsystem, sensing array, and the TDM receiver [11]. The optical pulse generator generates a low-duty cycle optical pulse with high ER. This is due to the distributed-feedback (DFB) laser diode source modulated by an OGW intensity modulator. An electrical pulse generator and a precision dc voltage supply are used to control the on-off modulation of the OGW. The sensing array consists of  $N$  sets of unbalanced sensing interferometer ( $SI_1, SI_2, \dots, SI_N$ ). Each SI consists of a fiber coupler (FC) and two FRM's. The lead fiber subsystem includes the input-output lead fibers, a three-port optical circulator (3POC), a post-EDFA and an in-line EDFA. The TDM receiver includes a CI, an optical receiver, time delay generator, sample/hold circuits and the phase-generated carrier (PGC) demodulator [12].

All path difference ( $\Delta L = 10$  m) are equal for all unbalanced sensing interferometers and the CI. In general, the output power of each sensor is required to be equal. The power splitting ratios among all fiber couplers ( $FC_1, FC_2, \dots, FC_N$ ) are 1:1 in order to maximize the visibility of the output intensity for each sensor. The power splitting ratios  $X_m$  of series fiber couplers ( $C_N, C_{N-1}, \dots, C_2$ ) are different in order to obtain equalized output power for every sensor. The  $X_m$  (here,  $2 \leq m \leq N$ ) has been derived and calculated in [7].

In the experiments, the EDFA is placed at three different positions within the TDM-PIFOMIS system: 1) as a postamplifier between the OGW and the sensing array (i.e., located at input lead fiber), 2) as an in-line amplifier between the sensing array and the CI (i.e., located at output lead fiber), and 3) as a preamplifier between the CI and the optical receiver.

A high-power ( $\sim 10$  mW) long wavelength ( $\sim 1.55$   $\mu$ m) DFB laser is chosen as a CW light source with a 3-dB linewidth of 1 MHz. A LiNbO<sub>3</sub> OGW intensity modulator (insertion loss  $\sim 6$  dB), controlled by a pulse generator and

a precision dc voltage supply, is used to generate the optical pulse with an optimum ER of about 33 dB (the optimum ER is limited by the performance of the OGW). The pulse repetition rate and pulse width are 880 kHz and 80 ns, respectively. An InGaAs PIN optical receiver of the New Focus (model 1811) is used in the TDM receiver for converting the interfered pulse trains into electrical signals. The CW saturation power and the maximum pulse power at 1.55  $\mu$ m of this receiver are about 60  $\mu$ W and 5 mW, respectively. Its conversion gain is about  $4 \times 10^4$  V/W. The sample/hold circuits include the AD9100 track/hold amplifier with a settling time of 20 ns for high-sampling rate and low-distortion signal processing. We find that in the preamplifier case, the EDFA has limited usefulness owing to the unstable amplification for the optical pulse trains with interference signals (i.e., the unstable optical gain of EDFA is induced by the fluctuated input light intensity). These amplitudes of the optical pulse trains that propagated in the output lead fiber of the TDM-PIFOMIS system are stable (there are not interference signal yet); therefore, they would be stable after amplified by the in-line EDFA. Furthermore, the in-line amplifier with stable optical gain of the EDFA in this system, located before the CI, is better to replace the preamplifier. Hence, we emphasize our investigation on the performance of the post- and the in-line amplifier cases.

Note that only the first sensor  $SI_1$  and the CI are used in all experiments for the feasibility study. Furthermore, during our experiments, the  $SI_1$  and CI are placed inside a vibration-isolated, acoustic-shielded box to avoid any ambient perturbations. An optical bandpass filter (OBPF) is connected behind the EDFA to filter out the ASE noise from the EDFA. The OBPF has a 0.5 dB bandwidth of 1 nm and an insertion loss of about 1.5 dB.

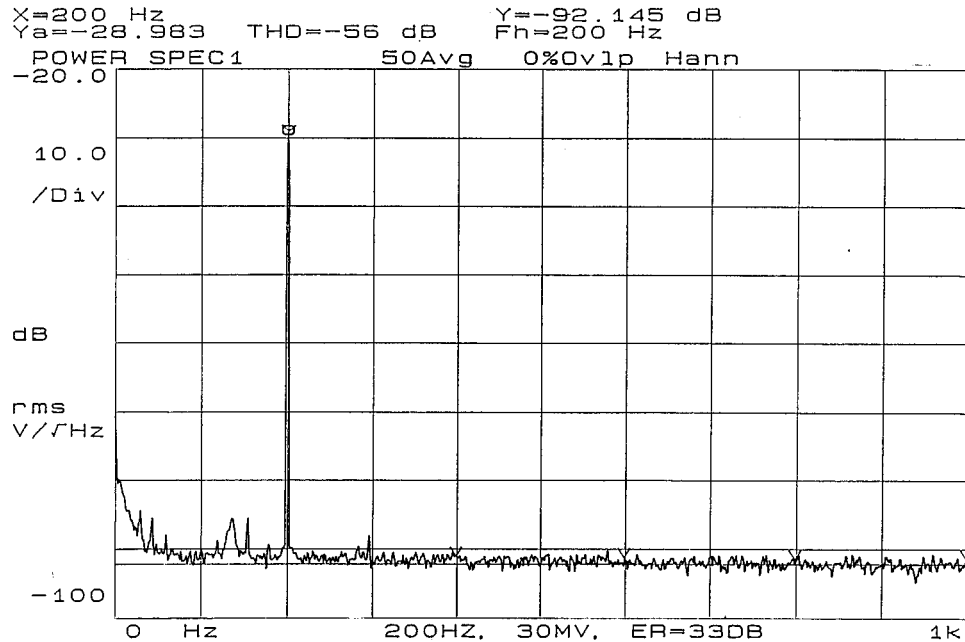


Fig. 2. The output spectrum of the demodulated signal at 200 Hz with the ER = 33 dB of the input optical pulse and without EDFA in the system.

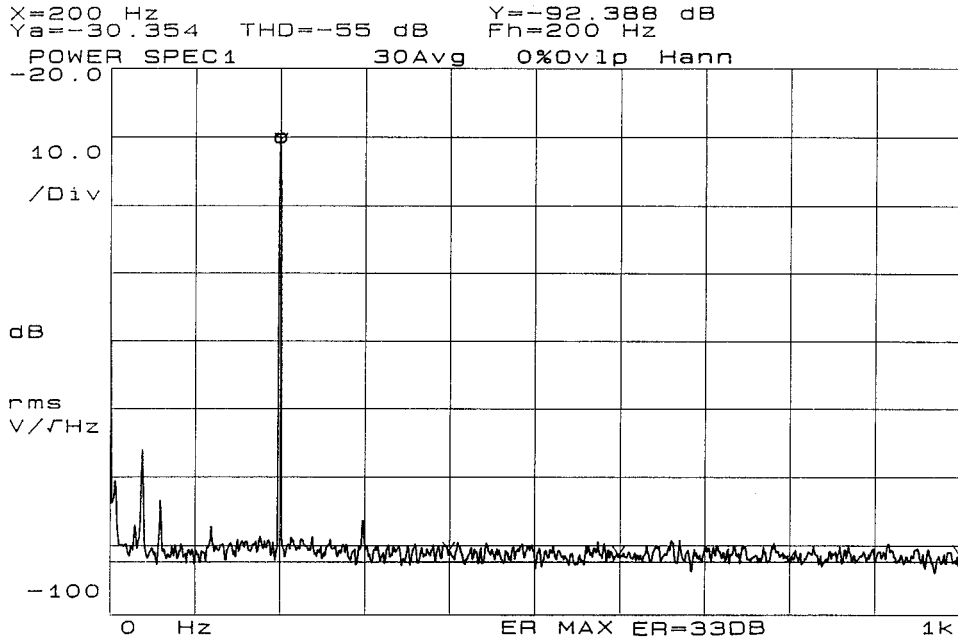


Fig. 3. The output spectrum of the demodulated signal at 200 Hz for a post-EDFA and an OBPF used in the system when the peak power and the ER of the input optical pulse are  $-5$  dBm and 33 dB.

### B. Experiment Results

In the experiments, the specific tested sensing signal of 200 Hz, generated by a signal generator, is applied upon one of the sensor's fiber arm through a PZT phase modulator to provide an effective phase signal of  $3.4 \times 10^{-2}$  rad/(Hz) $^{1/2}$ . A carrier signal of 20 kHz, generated by another signal generator, is applied upon one of the CI's fiber arm through a PZT phase modulator to provide an optimum phase of 2.37 rad for PGC demodulation. The interference pulse trains are detected by the receiver and the sensing signal is demodulated by the PGC demodulator. The detailed processes have been described in [11]. Some experimental results for EDFA used as a post- and an in-line amplifier

are obtained in [11]. In this paper, the influence of the ER of the optical pulse from the OGW output and the effect of the ASE of the EDFA in the system was investigated. The ER of an optical pulse can be calculated by

$$ER = 10 \log(P_H/P_L) = 10 \log(V_H/V_L) \quad (1)$$

here  $P_H$  and  $P_L$  are high-level and low-level light powers of the optical pulse,  $V_H$  and  $V_L$  are the voltages of the optical pulse. In our experiment, the maximum ER of the optical pulse from the OGW output is about 33 dB and can be automatically adjusted to the optimum condition [13].

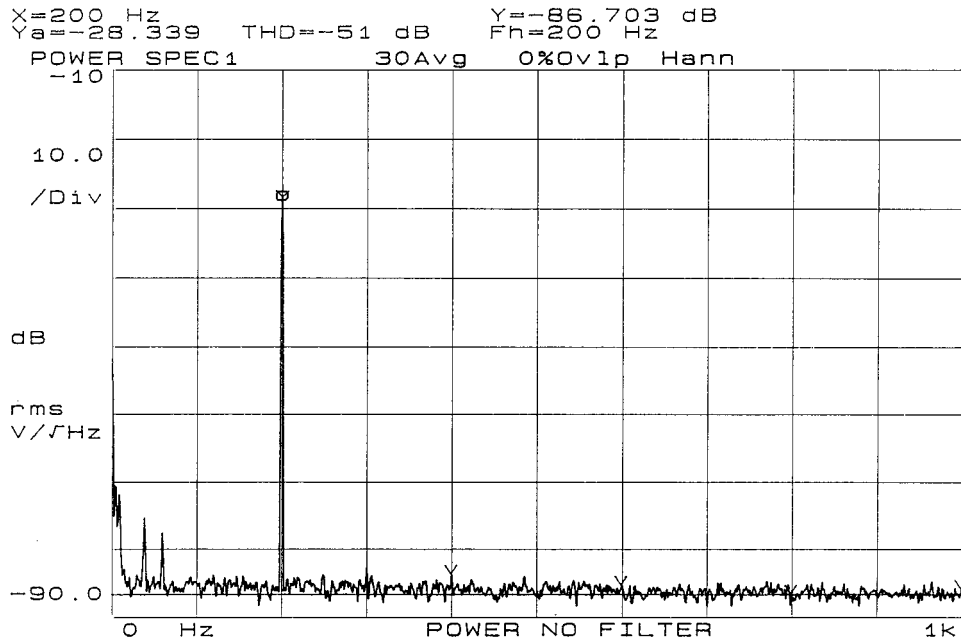


Fig. 4. The output spectrum of the demodulated signal at 200 Hz for a post-EDFA (without OBPF) used in the system when the peak power and the ER of the input optical pulse are  $-5$  dBm and 33 dB.

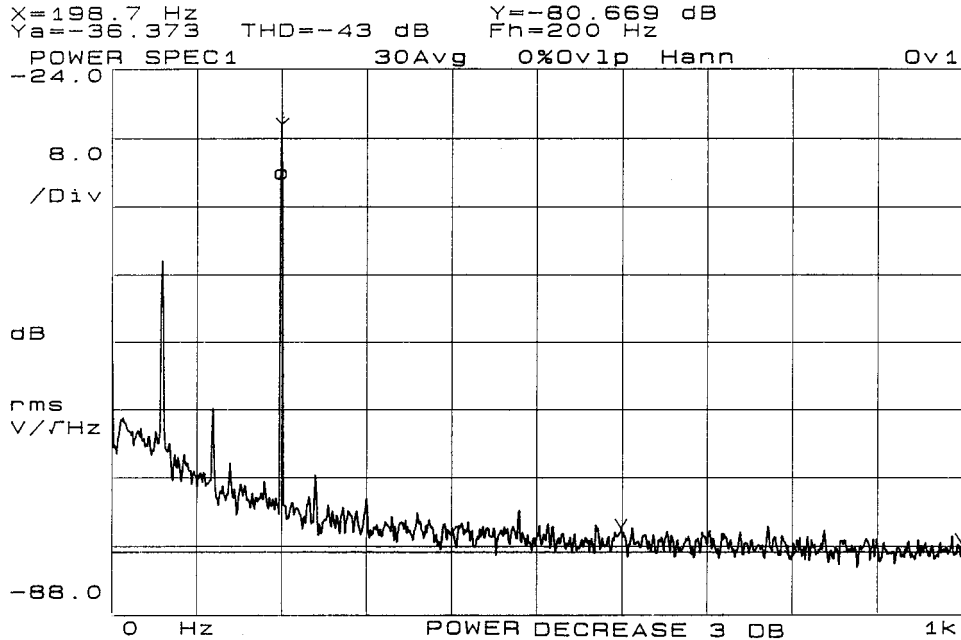


Fig. 5. The output spectrum of the demodulated signal at 200 Hz for a post-EDFA and an OBPF used in the system when the peak power and the ER of the input optical pulse are  $-5$  dBm and 30 dB.

The HP3562A dynamic signal analyzer is used to measure the spectrum of demodulated sensing signal to examine the system relative system noise (RSN) at 1 kHz. Fig. 2 shows the output spectrum of the demodulated signal at 200 Hz when the ER of the optical pulse from the OGW output is 33 dB without EDFA in the TDM-PIFOMIS system. In Fig. 2 the noise contains the amplitude noise of the light source, PIIN, the acoustic and vibration induced noises from the environment. Through some kinds of noise reduction process for light source, acoustic and vibration, we recognized PIIN as the major contributor among all noise sources. This is the optimum condition to obtain the lowest

phase noise for the experimental system. The corresponding RSN is  $-63.2$  dB. This RSN value is used as an index to evaluate the system performance. Fig. 3 shows the output spectrum for the system with post-EDFA and OBPF when the peak power is  $-5$  dBm and the ER of the optical pulse from the OGW output is 33 dB (the ER of the amplified optical pulse is 28 dB), RSN is  $-62$  dB. Fig. 4 shows the output spectrum for the system with post-EDFA (without OBPF) when the peak power is  $-5$  dBm and the ER of the optical pulse from the OGW output is 33 dB (the ER of the amplified optical pulse is 15 dB), RSN is  $-58.4$  dB. Fig. 5 shows the output spectrum for the system with

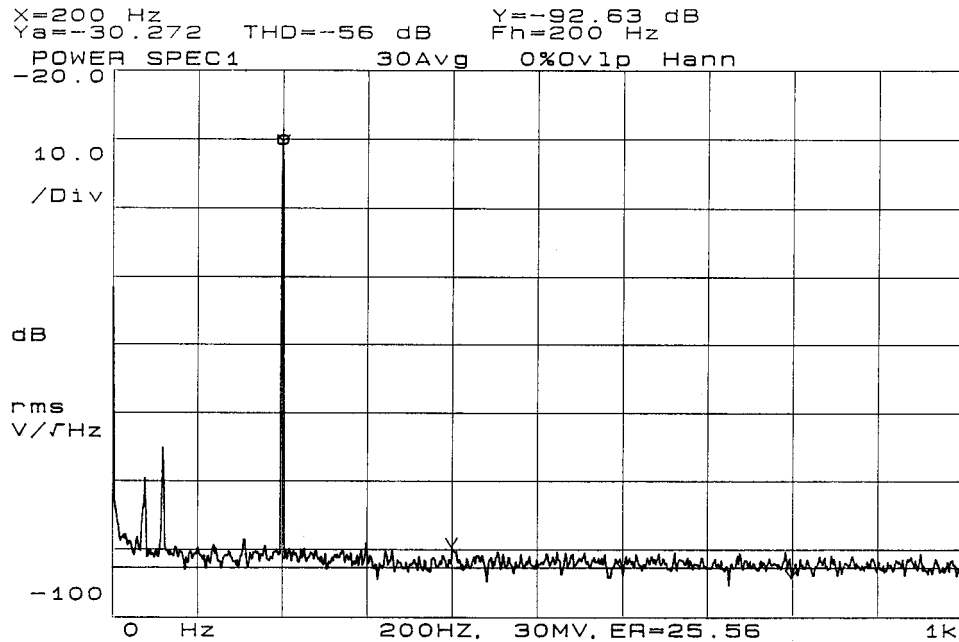


Fig. 6. The output spectrum of the demodulated signal at 200 Hz for an in-line EDFA and an OBPF used in the system when the peak power and the ER of the input optical pulse are  $-8.6$  dBm and 33 dB.

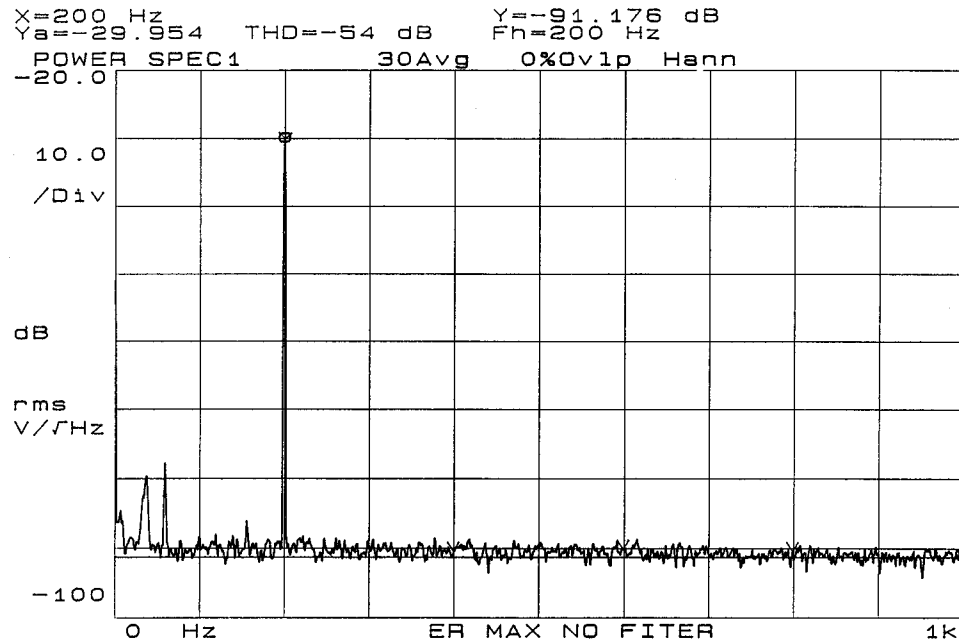


Fig. 7. The output spectrum of the demodulated signal at 200 Hz for an in-line EDFA (without OBPF) used in the system when the peak power and the ER of the input optical pulse are  $-8.6$  dBm and 33 dB.

post-EDFA and OBPF when the peak power is  $-5$  dBm and the ER of the optical pulse from the OGW output is 30 dB, RSN is  $-50.8$  dB. Fig. 6 shows the output spectrum for the system with in-line EDFA and OBPF when the peak power is  $-8.6$  dBm and the ER of the optical pulse from the OGW output is 33 dB (the ER of the amplified optical pulse is 25.6 dB), RSN is  $-62.4$  dB. Fig. 7 shows the output spectrum for the system with in-line EDFA (without OBPF) when the peak power is  $-8.6$  dBm and the ER of the optical pulse from the OGW output is 33 dB (the ER of the amplified optical pulse is 8.8 dB), its RSN is  $-61.2$  dB. Fig. 8 shows the output spectrum for the system with in-line

EDFA and OBPF when the peak power is  $-8.6$  dBm and the ER of the optical pulse from the OGW output is 30 dB, RSN is  $-49.4$  dB. In Figs. 3–8, the excess noise relative to that in Fig. 2, except a small amount induced by ASE from the EDFA needed further study, are definite attributed to PIIN.

The RSN shown in Fig. 2 for the unamplified TDM-PIFOMIS system (i.e., with the ER of 33 dB) is  $-63.2$  dB. The MPDS can be calculated from RSN by

$$\text{MPDS} = 3.4 \times 10^{-2} \times 10^{\text{RSN}/20} \text{ rad/(Hz)}^{1/2}. \quad (2)$$

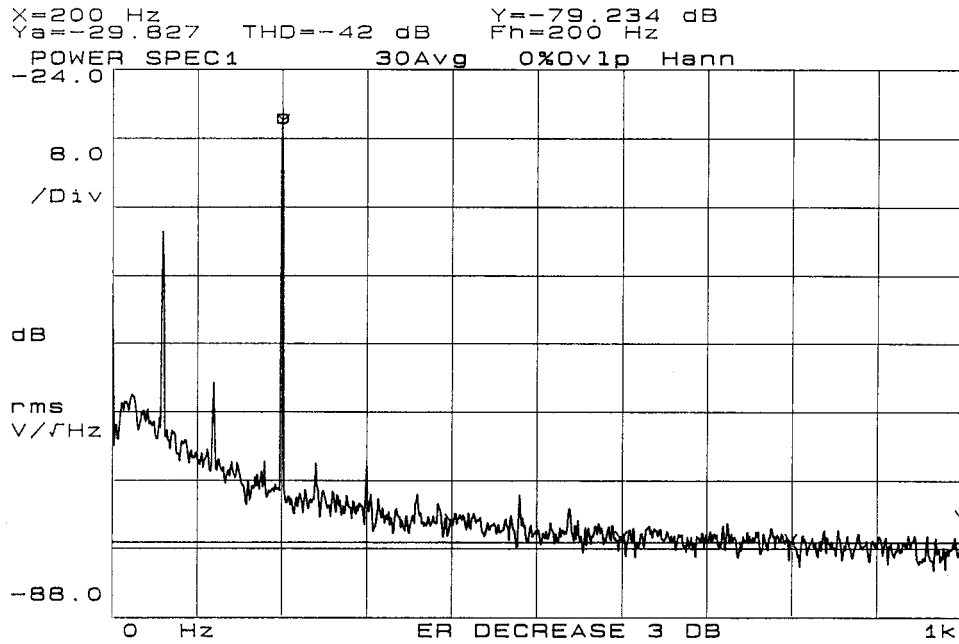


Fig. 8. The output spectrum of the demodulated signal at 200 Hz for an in-line EDFA and an OBPF used in the system when the peak power and the ER of the input optical pulse are  $-8.6$  dBm and 30 dB.

The MPDS of the unamplified TDM-PIFOMIS system (in this experimental system with one sensor) with ER of 33 dB is  $2.4 \times 10^{-5}$  rad/(Hz) $^{1/2}$  at about 1 kHz. To guarantee the optically amplified TDM-PIFOMIS system (with one sensor) operating with low-phase noise, it requires reasonably that the RSN limitation should not be 3 dB worse than that of the unamplified system. Thus the allowable maximum RSN level is about  $-60$  dB for the amplified system. That means the MPDS must be better than  $3.4 \times 10^{-5}$  rad/(Hz) $^{1/2}$  at about 1 kHz. To satisfy these requirements, the allowable worst ER for the post- and the in-line amplifier system are 20 and 17.8 dB, respectively (from [11, Fig. 14]). Thus, the minimum required peak power level of the input optical pulse for the post- and the in-line amplifier cases are  $-20$  and  $-25$  dBm, respectively (from [11, Fig. 13]). The corresponding output power levels are 9.5 and 6.9 dBm, respectively. In this condition, the optical gain for the post- and the in-line amplifier cases are 29.5 and 31.9 dB, respectively.

### III. PIIN OF THE OPTICALLY AMPLIFIED TDM-PIFOMIS SYSTEM

In the experiments, a high-frequency carrier is used for the PGC demodulation to prevent the demodulated sensing signal from the low-frequency intensity noise of the laser diode source. Therefore, the MPDS is mostly limited by the PIIN of the system. In the TDM-PIFOMIS system, assume that the time difference between two optical pulses (they can overlap through different paths to generate the interference signal) from laser emission is equal to  $\Delta t$ , and the laser diode source has a frequency instability  $dv_n$ .  $d\phi_n$  is the effective phase noise of the sensor of the system that comes from the PIIN that is given by [14]

$$d\phi_n = 2\pi\Delta t(dv_n). \quad (3)$$

In our experiments, the  $dv_n$  of the DFB-LD source with a linewidth of 1 MHz (coherence length  $L_C = 300$  m) approximates  $3$  kHz/(Hz) $^{1/2}$  at 1 kHz [14].

#### A. PIIN of the Unamplified TDM-PIFOMIS System with One Sensor

The PIIN of the unamplified TDM-PIFOMIS system with one sensor comes from two parts as follows:

1) *PIIN Due to Path Difference*: The path differences between two unbalanced arms of the above  $SI_1$  and  $CI$  are  $\Delta L_{S1}$  and  $\Delta L_{CI}$ , respectively. Ideally, the TDM-PIFOMIS system requires matched optical path between  $CI$  and  $SI_1$ , i.e.,  $\Delta L = \Delta L_{S1} = \Delta L_{CI}$ . In fact, the measured and cut processes for optical fiber often cause the error between  $\Delta L_{S1}$  and  $\Delta L_{CI}$ ,  $|\Delta L_{S1} - \Delta L_{CI}|$  is denoted as  $l$ . The effective phase noise  $d\phi_n$  comes from the PIIN, the  $d\phi_n$  generated by the path difference  $2l$  is given by

$$d\phi_n = 2\pi n(2l) dv_n/c. \quad (4)$$

Here  $c$  is light velocity and  $n$  is the index refraction of the optical fiber core. In our process of the sensing system, by means of a millimeter-resolution OTDR,  $l$  could be controlled within 2 mm. Assume that  $l$  is equal to 2 mm, then the  $d\phi_n$  due to path difference  $2l$  will be  $3.6 \times 10^{-7}$  rad/(Hz) $^{1/2}$  for the DFB-LD source with  $dv_n = 3$  kHz/(Hz) $^{1/2}$  at 1 kHz. In general, this is normal  $d\phi_n$  of the TDM-PIFOMIS system and is denoted as  $(d\phi_n)_{\text{normal}}$ .

2) *PIIN Due to Low-Level Light Power*: In the unamplified TDM-PIFOMIS system with one sensor, the low-level light power  $P_L$  of an optical pulse and the high-level light power  $P_H$  of the other optical pulse can interfere to induce the PIIN. In Fig. 1, at the output of the coupler  $FC_1$  of sensor  $SI_1$ , the high-level light power  $P_H$  of the optical pulse comes from one arm of sensor  $SI_1$ , while  $P_L$  comes from the other arm, at the

same time. The time difference  $\Delta t_L$  between  $P_L$  and  $P_H$  is equal to  $2n\Delta L/c$ . In this analysis, only the time difference of the two optical pulses of an interference term is needed. Hence, the phase information of the couplers in the TDM-PIFOMIS system isn't considered for simply analysis [15]. Assume that the electric field reflected by  $\text{FRM}_1$  and  $\text{FRM}'_1$  of  $\text{SI}_1$  are denoted as  $E_{H1}$  and  $E_{L1}$ ,  $E'_{H1}$  and  $E'_{L1}$ , respectively. Let  $E_H$  and  $E_L$  be the retraced electric field amplitudes of  $P_H$  and  $P_L$  at point A (between circulator 3POC and coupler  $C_N$ ), we can obtain the relation  $E_H/E_L = (P_L/P_H)^{1/2} = 10^{(-\text{ER}/20)}$ . These retraced electric fields at point A are

$$E_{H1} = E_H(0) = E_H \quad (5a)$$

$$E'_{H1} = E_H(0) \exp[i(\omega\Delta t_{S1})] = E_H \exp[i(\omega\Delta t_{S1})] \quad (5b)$$

$$E_{L1} = E_L(\Delta t_L) \exp[i(\omega\Delta t_L)] = E_L \exp[i(2\omega\Delta t_L)] \quad (5c)$$

$$\begin{aligned} E'_{L1} &= E_L(-\Delta t_L) \exp[i\omega(\Delta t_{S1} - \Delta t_L)] \\ &= E_L \exp[i\omega(\Delta t_{S1} - 2\Delta t_L)] \end{aligned} \quad (5d)$$

where  $\Delta t_{S1} = 2n\Delta L_{S1}/c$ ,  $\omega$  is the angular frequency of the laser source. The values 0 of  $E_H(0)$ ,  $\Delta t_L$  of  $E_L(\Delta t_L)$  and  $-\Delta t_L$  of  $E_L(-\Delta t_L)$  denote the different emitted time from laser. These electric fields propagate along the same path to the coupler  $\text{FC}_C$  and then couple to CI. The interference signal of  $\text{SI}_1$  is generated by CI, in which  $E'_{H1}$  and  $E_{L1}$  are reflected by  $\text{FRM}_C$  with the effective carrier phase signal  $2\phi_C$ , while  $E_{H1}$  and  $E'_{L1}$  are reflected by  $\text{FRM}'_C$  with the delay time  $\Delta t_{\text{CI}} = 2n\Delta L_{\text{CI}}/c$ . The  $2\phi_C$  is generated by the phase modulator PZT<sub>C</sub> for the PGC demodulation. Finally, these fields simultaneously propagate to the output (in front of the receiver) of the coupler  $\text{FC}_C$  with attenuation coefficient  $b$  (ideally, with the same attenuation) and are expressed as follows:

$$E_{H1} = bE_H \exp[i(\omega\Delta t_{\text{CI}})] \quad (6a)$$

$$E'_{H1} = bE_H \exp[i(\omega\Delta t_{S1} + 2\phi_C)] \quad (6b)$$

$$E_{L1} = bE_L \exp[i(2\omega\Delta t_L + 2\phi_C)] \quad (6c)$$

$$E'_{L1} = bE_L \exp[i\omega(\Delta t_{S1} - 2\Delta t_L + \Delta t_{\text{CI}})] \approx bE_L \quad (6d)$$

where  $\Delta t_{\text{CI}} \approx \Delta t_{S1} \approx \Delta t_L$ , therefore,  $\Delta t_{S1} - 2\Delta t_L + \Delta t_{\text{CI}} \approx 0$ . The total electric field  $E_T$  is

$$E_T = E_{H1} + E'_{H1} + E_{L1} + E'_{L1}. \quad (7)$$

The output intensity  $I_T$  of the interference signal is proportional to  $\langle E_T^* \cdot E_T \rangle$ . Let  $I_T = \eta \langle E_T^* \cdot E_T \rangle$ , where asterisk \* denotes a complex conjugation and  $\eta^{-1}$  is called wave impedance. If the

coherence length ( $L_C = 300$  m) of the laser source is much larger than  $2\Delta L$  (20 m), the total intensity  $I_T$  will be

$$\begin{aligned} I_T = & 2\eta b^2 [E_H^2 + E_L^2 + E_H^2 \cos(\omega t_l + 2\phi_C) \\ & + E_H E_L \cos(\omega\Delta t_L + 2\phi_C) + E_H E_L \cos(\omega\Delta t_L) \\ & + E_H E_L \cos(\omega\Delta t_L) + E_H E_L \cos(\omega\Delta t_L + 2\phi_C) \\ & + E_L^2 \cos(2\omega\Delta t_L + 2\phi_C)] \end{aligned} \quad (8)$$

where  $t_l = 2nl/c$ ,  $l = |\Delta L_{S1} - \Delta L_{\text{CI}}|$ ,  $\Delta t_{\text{CI}} \approx \Delta t_{S1} \approx \Delta t_L$ . The last six terms in brackets of (8) are interference signals. The first interference term  $E_H^2 \cos(\omega t_l + 2\phi_C)$  includes amplitude  $E_H^2$ , path difference  $2l$ , and carrier phase signal  $2\phi_C$ . The effective phase noise  $d\phi_n$  due to this term through the PGC demodulation has been analyzed as (4) and denoted as  $(d\phi_n)_{\text{normal}}$ . The second and fifth interference terms  $E_H E_L \cos(\omega\Delta t_L + 2\phi_C)$  include amplitude  $E_H E_L$ , time delay  $\Delta t_L$  of the two-interference optical pulses (included the different emitted time from laser) and carrier phase signal  $2\phi_C$ . The  $d\phi_n$  due to this interference term through the PGC demodulation is given by

$$\begin{aligned} d\phi_n &= \frac{2\pi n(2\Delta L)dv_n}{c} \frac{E_L}{E_H} = \frac{\Delta L}{l} \frac{E_L}{E_H} (d\phi_n)_{\text{normal}} \\ &= \frac{\Delta L}{l} 10^{(-\text{ER}/20)} (d\phi_n)_{\text{normal}}. \end{aligned} \quad (9)$$

In this experiment,  $\Delta L = 10$  m,  $\text{ER} \approx 33$  dB,  $l \approx 2$  mm. The  $d\phi_n$  of (9) can be calculated as  $d\phi_n \approx 112(d\phi_n)_{\text{normal}} = 4 \times 10^{-5}$  rad/(Hz)<sup>1/2</sup> at 1 kHz. The third and fourth interference terms do not include the carrier phase signal  $2\phi_C$ , so that no PIIN induced [12]. The last interference term  $E_L^2 \cos(2\omega\Delta t_L + 2\phi_C)$  can be neglected because of its small amplitude  $E_L^2$  ( $\approx 5 \times 10^{-4} E_H^2$ ).

The effective phase noise  $d\phi_n$  (that comes from the PIIN) induced from an interference term is proportional to the square root of the optical noise power. In the interferometer for sensing application with a small bandwidth (compared to  $c/(nD)$ ,  $D$  is path difference) and the coherence length  $L_C \gg D$ , the optical noise power of an interference term is proportional to  $I_1 I_2 D^2 / L_C$  ( $I_1$  and  $I_2$  are light intensities of two interference beams) [16]. The  $d\phi_n$  induced from an interference term is proportional to  $(I_1 I_2)^{1/2} D$ , this result corresponds with (4) (proportional to  $D$ ). The total PIIN is proportional to the square root of total optical noise power of all effective interference terms (with carrier phase signal  $2\phi_C$ ). Therefore, the total  $d\phi_n$  induced from (8) can be calculated as  $(d\phi_n)_{\text{total}} \approx [2 \times (112)^2 + 1]^{1/2} (d\phi_n)_{\text{normal}} \approx 158(d\phi_n)_{\text{normal}} = 5.7 \times 10^{-5}$  rad/(Hz)<sup>1/2</sup> for the DFB laser source with the  $dv_n = 3$  kHz/(Hz)<sup>1/2</sup> at 1 kHz.

#### B. PIIN of the Unamplified TDM-PIFOMIS System with $N$ Sensors

In the unamplified TDM-PIFOMIS system with  $N$  sensors, the low-level light power  $P_L$  of the optical pulse is unwanted light power. The sensor crosstalk due to  $P_L$  has been analyzed in [7].  $P_L$  of an optical pulse of a sensor and  $P_H$  of an optical pulse of the other sensor can interfere also to induce the PIIN. Therefore, the PIIN of a sensor of the unamplified TDM-PIFOMIS system with  $N$  sensors comes from 1) the self-PIIN of the sensor

(i.e., the PIIN of the unamplified TDM-PIFOMIS system with one sensor) and 2) the PIIN due to all  $(P_H, P_L)$  interferences among sensors. Here, the 2) term will be analyzed.

In Fig. 1, consider the PIIN of the  $i$ th sensor comes from the interference of the  $j$ th sensor, i.e., the PIIN due to the interference from  $P_H$  of the  $i$ th sensor and  $P_L$  of the  $j$ th sensor. Let  $k = |j - i|$  (the PIIN only depends on  $|j - i|$ , we can assume  $j > i$  for the analysis), the time difference between the  $i$ th sensor and the  $j$ th sensor is equal to  $2nk\Delta L/c = k\Delta t_L$ . These PIIN's can be caused by two situations. The first one occurs when two  $P_L$  reflected by  $\text{FRM}_j$  and  $\text{FRM}_{j'}$  of  $SI_j$  and the  $P_H$  reflected by  $\text{FRM}_i$  of  $SI_i$  propagate to coupler FC simultaneously. The second situation is similar to the first, but  $\text{FRM}_i$  is replaced by  $\text{FRM}_{i'}$  of  $SI_i$ . In the first situation, we assume that  $E_{Lj}$  and  $E'_{Lj}$  are electric fields of  $P_L$  reflected by  $\text{FRM}_j$  and  $\text{FRM}_{j'}$  of  $SI_j$ , respectively, while  $E_{hi}$  and  $E'_{hi}$  are electric fields of  $P_H$  reflected by  $\text{FRM}_i$  and  $\text{FRM}_{i'}$  of  $SI_i$ , respectively. These retraced electric fields at point A (between circulator 3POC and coupler  $C_N$ ) are

$$E_{hi} = E_{Hi}(0) = E_H \quad (10a)$$

$$E'_{hi} = E_H(0) \exp[i(\omega\Delta t_{Si})] = E_H \exp[i(\omega\Delta t_{Si})] \quad (10b)$$

$$E_{Lj} = E_L(-k\Delta t_L) = E_L \exp[i(-\omega k\Delta t_L)] \quad (10c)$$

$$E'_{Lj} = E_L[-(k+1)\Delta t_L] = E_L \exp[-i\omega(k+1)\Delta t_L]. \quad (10d)$$

These electric fields propagate along the same path to the coupler  $FC_C$  and then couple to CI. The interference signal of  $SI_i$  is generated by CI, in which  $E'_{hi}$  is reflected by  $\text{FRM}_C$  with the effective carrier phase signal  $2\phi_C$ , while  $E_{hi}$ ,  $E_{Lj}$ , and  $E'_{Lj}$  are reflected by  $\text{FRM}_{C'}$  with the delay time  $\Delta t_{CI} = 2n\Delta L_{CI}/c$ . Finally, these fields simultaneously propagate to the output (in front of the receiver) of the coupler  $FC_C$  with attenuation coefficient  $b$  (ideally, we can assume same attenuation) and are expressed as follows:

$$E_{hi} = bE_H \exp[i(\omega\Delta t_{CI})] \quad (11a)$$

$$E'_{hi} = bE_H \exp[i(\omega\Delta t_{Si} + 2\phi_C)] \quad (11b)$$

$$E_{Lj} = bE_L \exp[i\omega(\Delta t_{CI} - 2k\Delta t_L)] \quad (11c)$$

$$E'_{Lj} = bE_L \exp[i\omega(\Delta t_{CI} - (2k+1)\Delta t_L)]. \quad (11d)$$

In the second situation, we use similar analytic procedures and obtain  $E_{Lj} = bE_L \exp[i\omega(-(2k-1)\Delta t_L + 2\phi_C)]$  and  $E'_{Lj} = bE_L \exp[i\omega(-2k\Delta t_L + 2\phi_C)]$ . Therefore, the complete electric fields  $E_{Lj}$  and  $E'_{Lj}$  are

$$E_{Lj} = bE_L \exp[i\omega(\Delta t_{CI} - 2k\Delta t_L)] + bE_L \exp[i\omega(-(2k-1)\Delta t_L + 2\phi_C)] \quad (12a)$$

$$E'_{Lj} = bE_L \exp[i\omega(\Delta t_{CI} - (2k+1)\Delta t_L)] + bE_L \exp[i\omega(-2k\Delta t_L + 2\phi_C)]. \quad (12b)$$

The total electric field  $E_T$  is

$$E_T = E_{hi} + E'_{hi} + E_{Lj} + E'_{Lj}. \quad (13)$$

The effective intensity  $I_{\text{eff}}$  includes the interference terms only corresponding to these two conditions is following: 1) contained the carrier phase signal  $2\phi_C$  and 2) the product of the electric field is  $E_H^2$  or  $E_H E_L$ . According to the PGC demodulation

theory, the PIIN is primarily due to the interference terms of the effective intensity  $I_{\text{eff}}$  given by

$$\begin{aligned} I_{\text{eff}} = & 2\eta b^2 [E_H^2 \cos(\omega t_l + 2\phi_C) \\ & + E_H E_L \cos(2\phi_C + 2\omega k\Delta t_L) \\ & + E_H E_L \cos(2\phi_C - 2\omega k\Delta t_L) \\ & + E_H E_L \cos(2\phi_C + \omega(2k+1)\Delta t_L) \\ & + E_H E_L \cos(2\phi_C - \omega(2k+1)\Delta t_L)]. \end{aligned} \quad (14)$$

The effective phase noise  $d\phi_n$  due to the first term of (14) has been analyzed as (4) and denoted as  $(d\phi_n)_{\text{normal}}$ . The second and third terms include time delay  $2k\Delta t_L$  of the two-interference optical pulses (included the different emitted time from laser). The  $d\phi_n$  due to this interference term through the PGC demodulation is given by

$$\begin{aligned} d\phi_n = & \frac{2\pi n(4k\Delta L)dv_n}{c} \frac{E_L}{E_H} \\ = & \frac{2k\Delta L}{l} 10^{(-\text{ER}/20)} (d\phi_n)_{\text{normal}}. \end{aligned} \quad (15)$$

In this experiment,  $\Delta L = 10$  m,  $\text{ER} \approx 33$  dB,  $l \approx 2$  mm. The  $d\phi_n$  of (15) can be calculated as  $d\phi_n \approx 2k[112(d\phi_n)_{\text{normal}}] = 2k[4 \times 10^{-5} \text{ rad}/(\text{Hz})^{1/2}]$  at 1 kHz. The  $d\phi_n$  due to the fourth and fifth terms are  $(2k+1)[112(d\phi_n)_{\text{normal}}]$ . For the simply analysis, the last five interference terms of (14) can approach  $2k[112(d\phi_n)_{\text{normal}}]$ .

The  $d\phi_n$  of a sensor of the unamplified TDM-PIFOMIS system with  $N$  sensors dependent on its position, the  $d\phi_n$  of the sensor located at middle position is less than that located at both ends in the array. Assume  $N = 8$ , the  $d\phi_n$  of the sensor located at the first position is calculated as

$$\begin{aligned} (d\phi_n)_{\text{total}} &= \left[ \left( 2 + 4 \times \sum_{k=1}^7 (2k)^2 \right) \times (112)^2 + 1 \right]^{1/2} (d\phi_n)_{\text{normal}} \\ &= 1.9 \times 10^{-3} \text{ rad}/\sqrt{\text{Hz}} \end{aligned} \quad (16)$$

for  $\Delta L = 10$  m,  $\text{ER} \approx 33$  dB,  $l \approx 2$  mm and the DFB laser source with the  $dv_n = 3 \text{ kHz}/(\text{Hz})^{1/2}$  at 1 kHz. The  $d\phi_n$  of the sensor located at fourth position ( $N = 8$ ) is  $(d\phi_n)_{\text{total}} = 1.1 \times 10^{-3} \text{ rad}/\sqrt{\text{Hz}}$ .

#### C. PIIN of the Amplified TDM-PIFOMIS System with $N$ Sensors

The effective phase noise  $d\phi_n$  (comes from the PIIN) of the amplified TDM-PIFOMIS system with  $N$  sensors comes from two parts: 1) due to the unamplified TDM-PIFOMIS system with  $N$  sensors and 2) due to post- and in-line EDFA. The post- and in-line EDFA in the amplified TDM-PIFOMIS system will degrade the ER of the amplified optical pulse because of ASE that adds noise to the optical pulse during its amplification. Most ASE due to the EDFA can be filtered out by a narrow OBPF. It is found that the ER of the amplified optical pulse of the post-EDFA will degrade at least 5 dB even the peak power of the input optical pulse is large enough, but the system RSN almost not degrade. We can assume that the effective ER of the amplified optical pulse of the EDFA will not degrade (i.e., the ER of the amplified optical pulse will not degrade in the narrow

linewidth such as 1 MHz). In the above condition,  $P_L$  includes residual ASE with coherence length  $L_C \ll 2\Delta L$ , ASE and  $P_H$  cannot interfere in path difference  $2\Delta L$  to increase the PIIN. When the peak power of the input optical pulse is small to degrade the effective ER of the amplified optical pulse of the EDFA, the system RSN will obviously degrade. Therefore, the PIIN of the amplified TDM-PIFOMIS system due to EDFA is dependent on the peak power of the input optical pulse. According to the experimental results, when the peak power of the input optical pulse is large enough and the ASE of the amplified optical pulse of the EDFA is filtered out by suitable OBPF, the PIIN of the amplified TDM-PIFOMIS system due to the EDFA can be neglected. In the optimum condition, the  $d\phi_n$  of the optically amplified system approximates to the  $d\phi_n$  of the unamplified system.

The detailed theoretical analysis of the amplified TDM-PIFOMIS system is very complicated, because the ASE from the EDFA depends on the intensity, pulse width, duty cycle and ER of the input light pulse. The signal-spontaneous beatnoise may plays an important role in our system, especially for the peak power of the input optical pulse is small. We will study this further in the future; however, in this paper, because the key issue is system design of the sensor system, the effect of the ASE from the EDFA in the system is directly quoted from the experimental results.

#### IV. SYSTEM DESIGN AND DISCUSSIONS

According to the theoretical analysis, the effective phase noise  $d\phi_n$  (comes from the PIIN) of the experimental system with ER = 33 dB is  $5.7 \times 10^{-5}$  rad/(Hz) $^{1/2}$  at 1 kHz and is primarily due to  $P_L$ . The  $d\phi_n$  (or MPDS) of the experimental result is  $2.4 \times 10^{-5}$  rad/(Hz) $^{1/2}$ , that is less than  $5.7 \times 10^{-5}$  rad/(Hz) $^{1/2}$ . There is a portion of  $P_L$  of the light pulse comes from the spontaneous emission light (SEL) of the laser diode, because of the broadband spectral character of the SEL, OGW cannot do effective on-off modulation to it.  $P_L$  includes some SEL of the laser with coherence length  $L_C \ll 2\Delta L$ , SEL and  $P_H$  cannot interfere in path difference  $2\Delta L$  to increase the PIIN, therefore, the  $d\phi_n$  of the experimental result is less than the theoretical result. When the ER of the output optical pulse of the OGW is adjusted to decrease 3 dB (i.e., ER = 30 dB) from the optimum condition and the peak power of the input signal is -5 dBm for the EDFA as a postamplifier, the output spectrum is shown in Fig. 5 and the MPDS is  $1 \times 10^{-4}$  rad/(Hz) $^{1/2}$  at 1 kHz. In this condition, the increased light power of  $P_L$  is totally lasing with coherence length  $L_C = 300$  m, when ER = 30 dB, the effective coherent light of  $P_L$  is excess twice the value as that when ER = 33 dB. Therefore, the experimental value of  $d\phi_n$  is  $1 \times 10^{-4}$  rad/(Hz) $^{1/2}$  that approximates the theoretical value  $8.2 \times 10^{-5}$  rad/(Hz) $^{1/2}$ . The same result is obtained in the system using the in-line EDFA. It is found that the value of the MPDS increases rapidly when the ER of the output optical pulse of the OGW decreased. Therefore, to select an OGW with high ER (typical ER  $\geq 30$  dB) and to control the output optical pulse of the OGW with optimum ER are very important in the TDM-PIFOMIS system.

The ASE of the optically amplified TDM-PIFOMIS system using post-EDFA degrade the RSN larger than that using an in-line EDFA about 2.8 dB from the experimental results. The reason is because the amplified optical pulse of the post-EDFA propagates through the sensor array causes some additional PIIN. Therefore, connected an OBPF to the output of the post-EDFA for reducing the PIIN is better than used an OBPF in the in-line EDFA. In general, only two OBPF's are needed: one located at the output of the series post-EDFA's and the other at the output of the series in-line EDFA's in the optically amplified TDM-PIFOMIS system for reducing the PIIN.

The  $P_L$  of an EDFA output increased when the input optical pulse power decreased which was mostly of ASE. We expect that the experimental value of  $d\phi_n$  is obviously less than the theoretical value in the optically amplified TDM-PIFOMIS system. For example, the ER of the amplified optical pulse is 20 dB for the post-EDFA, the  $d\phi_n$  is  $3.4 \times 10^{-5}$  rad/(Hz) $^{1/2}$  which is less than its theoretical value  $2.7 \times 10^{-4}$  rad/(Hz) $^{1/2}$  (from [11, Fig. 14]). When the peak power of the input optical pulse is large enough and the ASE of the amplified optical pulse of the EDFA is filtered out by a suitable OBPF, the PIIN of the amplified TDM-PIFOMIS system due to the EDFA can be neglected. According to the theoretical analysis, the  $d\phi_n$  of the optically amplified TDM-PIFOMIS system is proportional to  $\Delta L d\phi_n 10^{(-ER/20)}$ . In the future, if we use  $\Delta L = 4$  m, a commercial fiber laser source with linewidth about 10 kHz and the ER of an OGW about 33 dB, the MPDS of the amplified TDM-PIFOMIS system with eight sensors is expected to less than  $8 \times 10^{-6}$  rad/(Hz) $^{1/2}$ .

In this paper and [11], the experimental results have shown the feasibility of using EDFA's in the PGC-demodulated TDM-PIFOMIS system as a post- and an in-line amplifier. The EDFA, especially for the in-line case, does not degrade the interference signal of the sensor system. However, the amplitudes of the optical pulse trains are very stable after amplified by the in-line EDFA amplifier. This is a significantly advantage of the optically amplified TDM-PIFOMIS system. The excess power budget can effectively increase the number of sensors and transmission distance for field application. In practice, the TDM-PIFOMIS array systems may have several tens of sensors and hundreds of kilometers long of lead-fiber.

In the optically amplified TDM-PIFOMIS system, the upper limit of the allowable number of sensors is determined by the condition that a postamplifier and an in-line amplifier, are located at the input port 1 and the output port 3 of the 3POC in front of the sensing array, respectively. The present TDM-PIFOMIS system requires that the MPDS be better than  $3.4 \times 10^{-5}$  rad/(Hz) $^{1/2}$  at 1 kHz, the minimum required peak power level of the input pulse for the in-line amplifier is -25 dBm. The peak power -5 dBm of the input pulse for the postamplifier is required to obtain the peak output power 22 dBm. Then the amplified output peak powers of the post- and in-line amplifiers for the aforesaid input peak powers are 22 and 7 dBm, respectively. Therefore, the allowable total loss of the sensing array (the one-way insertion loss of the optical circulator of 1 dB is included) can reach 47 dB (= 22 + 25 dB). Using [8, eq. (45)] with this loss and the related parameter values, the upper limit of the allowable number of sensors for the system with these am-

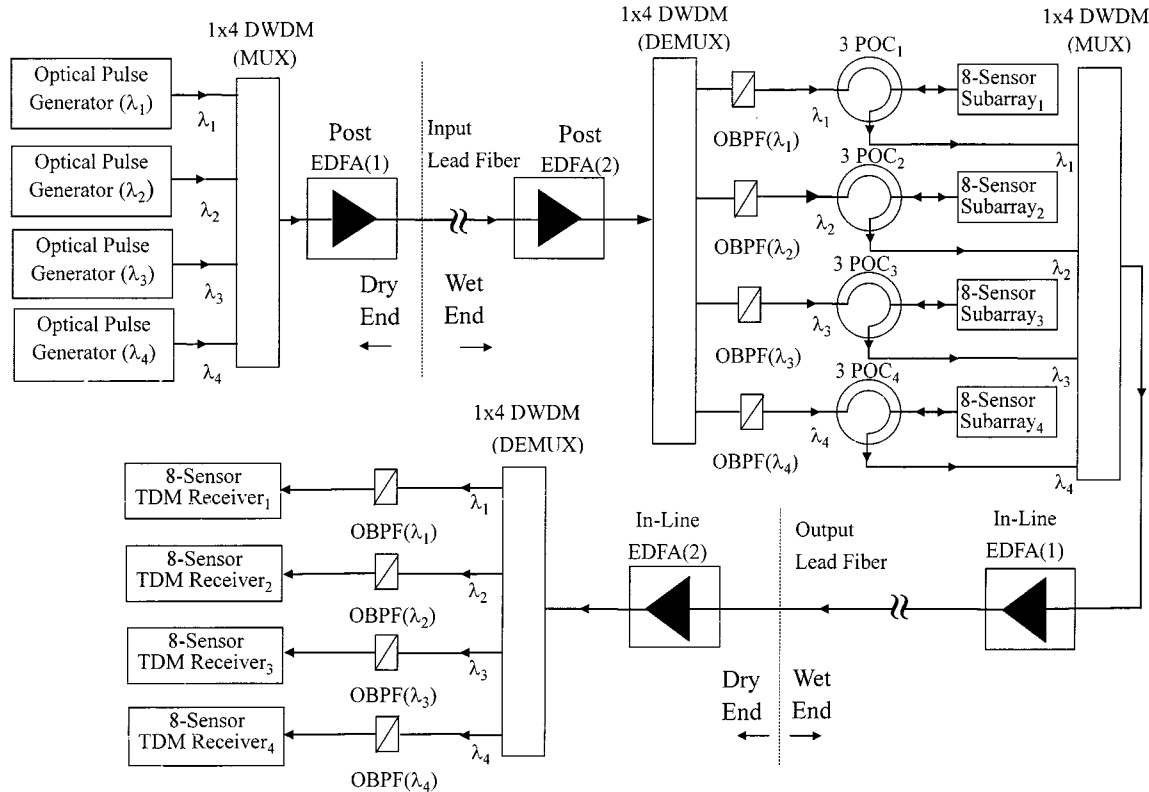


Fig. 9. WDM (four wavelengths)-TDM hybrid PIFOMIS system with a 32-sensor array, while employing two post- and two in-line EDFA's.

plifiers is 32. In the calculations, the single-pass insertion loss of the FRM, 3POC, and 3 dB-coupler are 1, 1, and 3 dB, respectively. The excess loss of the 3 dB coupler is 0.2 dB. Considering the settling time of the high-resolution sample/hold circuit, to demodulate the pulse trains of a 32-sensor array successfully will be a challenge. Additionally, the PIIN of the optically amplified TDM-PIFOMIS system with large number sensors will obviously be enlarged. So, utilization of sensor subarrays can simplify this problem. For an eight-sensor subarray system, the system loss is about 28 dB. Therefore, the 47-dB loss budget can realize a four-subarray (loss about 34 dB) TDM-PIFOMIS system with eight sensors per subarray. Hence, a  $1 \times 4$  fiber coupler with equal splitting ratio and four separate sets of 3POC, in-line amplifier, output lead fiber, and TDM optical receiver are required for such a four-subarray system. This may increase the system complexity and cost. In order to improve this system, we suggest a WDM-TDM hybrid PIFOMIS system as shown in Fig. 9 to replace the TDM-PIFOMIS system with subarray.

In Fig. 9, the outputs of four optical pulse generators with wavelengths  $\lambda_1$ ,  $\lambda_2$ ,  $\lambda_3$ , and  $\lambda_4$  are multiplexed by a four-channel dense wavelength-division multiplexer ( $1 \times 4$  DWDM) into the post-EDFA(1), then propagate through the input lead fiber to the post-EDFA(2). The output of the post-EDFA(2) is demultiplexed by a high-isolation  $1 \times 4$  DWDM as four outputs with wavelengths  $\lambda_1$ ,  $\lambda_2$ ,  $\lambda_3$ , and  $\lambda_4$ , respectively. Four outputs of the  $1 \times 4$  DWDM are connected with four OBPF's, respectively. Four outputs of the four OBPF's are used as input optical pulses of four eight-sensor subarrays and are circulated by four high-directivity 3POC's, respectively, and then are multiplexed into the in-line EDFA(1)

by a high-isolation  $1 \times 4$  DWDM. This arrangement can avoid the effect of the back-reflected optical power of the  $1 \times 4$  DWDM. The output of the in-line EDFA(1) propagates through the output lead fiber and the in-line EDFA(2) is then demultiplexed by a high-isolation  $1 \times 4$  DWDM as four outputs. These four outputs are filtered by four OBPF's to reduce the PIIN and the crosstalks among four optical sources, respectively. Finally, these four outputs are coupled into four CI's to generate interference signals and are demodulated by four TDM receivers, respectively. This WDM-TDM hybrid PIFOMIS system not only saves three in-line EDFA's and three output lead fibers, but also simplifies the construction of the sensor system and reduces the electrical power consumption.

The post-EDFA(1) is located at the output of the first  $1 \times 4$  DWDM while the post-EDFA(2) is located at the input of it. The input pulse peak powers for each wavelength of the post-EDFA(1) and the post-EDFA(2) required  $-5$  and  $-10$  dBm to obtain the output power  $16$  and  $9$  dBm, respectively. Then the power budget of  $26$  dB [ $=16$  dB  $- (-10$  dB)] can be used for a  $104$ -km-long input lead fiber. The insertion loss of a  $1 \times 4$  DWDM approximates  $2.5$  dB, the system loss of an eight-sensor subarray is about  $28$  dB; therefore, the input power for each wavelength of the in-line EDFA(1) is  $-24$  dBm (from  $9$  dB  $- 2.5 \times 2$  dB  $- 28$  dB), that matched the system requirement. The output power for each wavelength of the in-line EDFA(1) is  $2$  dBm (from  $8$  dB  $- 6$  dB) while the input power of the in-line EDFA(2) required about  $-25$  dBm, then the system power budget of  $27$  dB [ $=2$  dB  $- (-25$  dB)] can be used for a  $108$  km long output lead fiber. Consequently, while employing such two postamplifiers and two in-line amplifiers,

the 104-km-long input–output lead fiber can be realized for this WDM–TDM hybrid PIFOMIS system with a 32-sensor array.

For field applications, the lead fiber length of a sensor system may require hundreds of km. If the required lead fiber length is more than 104 km, this system must have some extra post-EDFA's and in-line EDFA's in the input and output lead fibers. On the other hand, the transmitted power of a long single-mode fiber (SMF) will be limited by the stimulated Brillouin scattering (SBS) effect [17]. This effect of an SMF can be evaluated by two parameters such as the linewidth  $\Delta v_B$  and the effective interaction length  $L_e$ . These two parameters are 16 MHz and 22 km at the 1.55  $\mu\text{m}$ , respectively [18]. For a 1.55  $\mu\text{m}$  CW laser source with linewidth less than 16 MHz, the estimated transmitted threshold power is about 3 dBm when the propagated fiber length is larger than 22 km. In the WDM–TDM hybrid PIFOMIS system, the duty cycle of the optical pulse propagated in the input lead fiber is only 1/17 for each wavelength; therefore, the threshold power of the SBS approximates 15 dBm for each wavelength. This is the upper limit output power of the post-EDFA for efficiently propagated in the input lead fiber. The duty cycle of the optical pulse propagated in the output lead fiber approximates 1. The threshold power is no more than 3 dBm for each wavelength; this is the upper limit output power of the in-line EDFA for efficiently propagated in the output lead fiber.

For a practical implementation, the acceptable noise must be determined by its application. In this paper, we proposed just some theoretical and experimental schemes for the potential user. Therefore, after some acceptable noise level was reasonably defined, the user can arranged a sophisticated system accordingly, with well-defined spectral linewidth of the laser source, ER of OGW and the operational constraints of the EDFA etc.

## V. CONCLUSION

In conclusion, we have investigated the optically amplified TDM-PIFOMIS systems, with PGC demodulation technique, using EDFA's in different positions. We find that the preamplifier has limited usefulness owing to its unstable amplification of the optical pulse trains. Although the ASE noise generated by an EDFA degrades the ER for small input signal, both post- and in-line EDFA's configurations can still work successfully. The amplitudes of the optical pulse trains are still very stable after amplified by the in-line EDFA. This is a significantly advantage of the optically amplified TDM-PIFOMIS system compared with other TDM sensor systems in which those optical pulse trains propagate in the output lead fiber with interference signals. The MPDS for the unamplified TDM-PIFOMIS system at about 1 kHz is obtained as  $2.4 \times 10^{-5} \text{ rad}/(\text{Hz})^{1/2}$ . For maintaining the MPDS better than  $3.4 \times 10^{-5} \text{ rad}/(\text{Hz})^{1/2}$ , the worst ER for the post- and in-line amplifier cases are 20 and 18 dB, respectively, and the corresponding input signal peak power should be larger than  $-20$  and  $-25$  dBm, respectively. While employing such two postamplifiers and two in-line amplifiers, the allowable loss of the sensing array 47 dB can be realized for this TDM-PIFOMIS system.

According to the theoretical analysis, the effective phase noise  $d\phi_n$  (or MPDS) of the optically amplified TDM-PIFOMIS system is primarily due to  $P_L$  of the optical pulse from

the OGW output, and is proportional to  $\Delta L d\phi_n 10^{(-\text{ER}/20)}$  (the ER of the OGW output pulse). To select an OGW with high ER (typical ER  $\geq 30$  dB) and to control the output optical pulse of the OGW with optimum ER in the TDM-PIFOMIS system are very important to minimize the PIIN and sensor crosstalk. The PIIN is increased rapidly when the number of the sensors is increased. If we use  $\Delta L = 4$  m, a fiber laser with linewidth about 10 kHz and the ER of an OGW about 33 dB, the MPDS of the amplified TDM-PIFOMIS system with eight sensors is expected to less than  $8 \times 10^{-6} \text{ rad}/(\text{Hz})^{1/2}$ . To reduce the system PIIN, complexity and cost, we suggest a WDM (four wavelengths)–TDM hybrid PIFOMIS system with a 32-sensor array, while employing two postamplifiers and two in-line amplifiers. The 104-km-link length of the input–output lead fiber can be realized in the WDM–TDM hybrid PIFOMIS system. To combine the aforesaid improvements, we can obtain an optimum optically amplified WDM–TDM hybrid PIFOMIS system with four wavelengths and four eight-sensor subarrays. This system can use extra post-EDFA's and in-line EDFA's in the input and output lead fiber, to extend the transmitted length to more than 104 km.

## REFERENCES

- [1] A. D. Kersey, "Recent progress in interferometric fiber sensor technology," in *Proc. SPIE Fiber Optic and Laser Sensors VIII*, R. P. Depaula and E. Udd, Eds, 1990, pp. 2–12.
- [2] ———, "Multiplexed fiber optic sensors," in *Distributed and Multiplexed Fiber Optic Sensors II—Proc. SPIE 1797*, J. P. Dakin and A. D. Kersey, Eds., 1993, pp. 161–185.
- [3] J. L. Brooks, B. Boslehi, B. Y. Kim, and H. J. Shaw, "Time-domain addressing of remote fiber-optic interferometric sensor arrays," *J. Lightwave Technol.*, vol. LT-5, pp. 1014–1023, 1987.
- [4] A. D. Kersey, M. J. Marrone, and M. A. Davis, "Polarization-insensitive fiber optic Michelson interferometer," *Electron. Lett.*, vol. 27, pp. 518–520, 1991.
- [5] M. Martinelli, "A universal compensator for polarization change induced by birefringence on a retracing beam," *Opt. Commun.*, vol. 72, pp. 341–344, 1989.
- [6] S. C. Huang, W. W. Lin, and M. H. Chen, "Time-division multiplexing of polarization-insensitive fiber-optic Michelson interferometric sensors," *Opt. Lett.*, vol. 20, pp. 1244–1246, 1995.
- [7] S. C. Huang, W. W. Lin, M. H. Chen, S. C. Hung, and H. L. Chao, "Crosstalk analysis and system design of time-division multiplexing of polarization-insensitive fiber-optic Michelson interferometric sensors," *J. Lightwave Technol.*, vol. 14, pp. 1488–1500, 1996.
- [8] A. Dandridge and A. B. Tveten, "Phase noise of single mode diode laser in interferometer system," *Appl. Phys. Lett.*, vol. 39, pp. 530–532, 1981.
- [9] S. C. Huang, W. W. Lin, and M. H. Chen, "Crosstalk analysis of time-division multiplexing of polarization-insensitive fiber optic Michelson interferometric sensors with 3  $\times$  3 directional coupler," *Appl. Opt.*, vol. 36, pp. 921–933, 1997.
- [10] P. Nash, "Review of interferometric optical fiber hydrophone technology," *Inst. Elect. Eng. Proc.—Radar. Sonar Navig.*, vol. 143, pp. 204–209, 1996.
- [11] Y. K. Chen, P. C. Law, and S. C. Huang, "Experimental investigation of optically amplified time-division-multiplexed polarization-insensitive fiber-optic Michelson interferometric sensor system," *Appl. Opt.*, vol. 37, pp. 6615–6622, 1998.
- [12] A. Dandridge, A. B. Tveten, and T. G. Giallorenzi, "Homodyne demodulation scheme for fiber optic sensors using phase generated carrier," *IEEE J. Quantum Electron.*, vol. QE-18, pp. 1647–1653, 1982.
- [13] S. C. Huang, J. S. Tsay, and W. W. Lin, "A control method to maintain the maximum extinction ratio of optical pulses from an intensity modulator," *Optic. Eng.*, submitted for publication.
- [14] A. Dandridge, A. B. Tveten, R. O. Miles, D. A. Jackson, and T. G. Giallorenzi, "Single-mode diode laser phase noise," *Appl. Phys. Lett.*, vol. 38, pp. 77–79, 1981.

- [15] R. C. Youngquist, L. F. Stokes, and H. J. Shaw, "Effects of normal mode loss in dielectric waveguide directional couplers and interferometers," *IEEE J. Quantum Electron.*, vol. QE-19, pp. 1888–1896, 1983.
- [16] B. Moslehi, "Analysis of optical phase noise in fiber-optic systems employing a laser source with arbitrary coherence time," *J. Lightwave Technol.*, vol. LT-4, pp. 1334–1351, 1986.
- [17] R. G. Smith, "Optical power handling capacity of low loss optical fibers as determined by stimulated Raman and Brillouin scattering," *Appl. Opt.*, vol. 11, pp. 2489–2494, 1972.
- [18] D. Cotter, "Observation of stimulated Brillouin scattering in low loss silica fiber at 1.3  $\mu$ m," *Electron. Lett.*, vol. 18, pp. 495–496, 1982.



**Shih-Chu Huang** received the B.S. and M.S. degree in physics from National Cheng Kung University and National Tsing Hua University, Taiwan, in 1977 and 1979, respectively, and the Ph.D. degree in electrical engineering from National Sun Yat-Sen University, Taiwan, in 1996.

Since 1979, he has been employed as an Assistant Scientist in Chung Shan Institute of Science and Technology. His research includes fiber-optic sensors and multiplexed sensor system.



**Jiunn-Song Tsay** received the B.S. and M.S. degree in electrical engineering from National Taiwan Institute Techonology, Taiwan, in 1985 and 1987, respectively.

Since 1987, he has been employed as an Assistant Scientist in Chung Shan Institute of Science and Technology. His research includes digital signal processing and microcontroller system.



**Wuu-Wen Lin** received the B.S. and M.S. degrees in physics from National Taiwan Normal University and National Cheng-Kung University, Taiwan, in 1972 and 1974, respectively, the M.S. degree in mechanics and structurals from the University of California at Los Angeles (UCLA), in 1980 and Ph.D. degree in mechanical engineering from UCLA, in 1986.

Since 1976, he has been employed as an Assistant Scientist in Chung Shan Institute of Science and Technology. He is currently a Senior Scientist and working in the area of fiber-optic sensors.



**Shorn-Chien Hung** received the B.S. and M.S. degree in physics and optics of science from National Cheng Kung University, National Central University, Taiwan, in 1986 and 1988, respectively.

Since 1988, he has been employed as an Assistant Scientist in Chung Shan Institute of Science and Technology. His research includes fiber-optic sensors and multiplexed sensor system.